Catalysis Today 137 (2008) 80–89

Contents lists available at ScienceDirect

Catalysis Today

journal homepage: www.elsevier.com/locate/cattod

High-temperature parallel screening of catalysts for the oxidative coupling of methane

Louis Olivier [a], Stéphane Haag [a], Helmut Pennemann [b], Christian Hofmann [b], Claude Mirodatos [a], Andre C. van Veen [a,1,*]

[a] University of Lyon, Institut de Recherches sur la Catalyse et l'Environnement de Lyon (UMR 5256, CNRS – Université Claude Bernard Lyon 1),
2 avenue Albert Einstein, 69626 Villeurbanne Cedex, France
[b] Institut für Mikrotechnik Mainz GmbH, Carl-Zeiss-Straße 18-20, 55129 Mainz, Germany

ARTICLE INFO

Article history:
Available online 24 April 2008

Keywords:
Parallel reactor
OCM
Temperature stability
Reactor design

ABSTRACT

The oxidative coupling of methane (OCM) was investigated with a specifically designed multi-channel device operating fixed-bed reactors at high temperature and atmospheric pressure. The device allows precise temperature measurement in each channel selected for analysis and possesses a quench cooling unit right after the reaction zone. Analysis is based on a mass spectrometer allowing a time resolution of only 3 s per analysis and 30 s per reactor channel. Successful screening is demonstrated using a reactant feed of O_2 and CH_4 diluted in Ar at flows between 100 and 166 mL/min per reactor channel. As expected, Li/MgO-based catalysts showed good initial performance, but rapid deactivation at 800 °C excludes their use in high-temperature applications. Good C_2 selectivity up to 80% and high yields up to 20% were observed for La/Sr/CaO catalysts. Even more interesting, no decline in performance was observed for those formulations identifying 10% La/20% Sr/CaO as best catalyst in an initial library. Screening of various La and Sr loadings at different operating conditions identified a optimal content of 5–10% for La and 20% for Sr. The exploration of operating conditions showed increasing C_2 productivities with increasing reactant partial pressure, reaching at 800 °C values up to 1.3×10^{-5} mol $(C_2)\, s^{-1}\, g(cat)^{-1}$.

1. Introduction

The valorization of natural gas for chemical production was subject of extensive research in recent years, especially in view of recent high oil prices. Focusing on methane as main constituent, an exploitation in current chemical plants meets considerable obstacles like gas transport via a new pipeline infrastructure or by liquefaction requiring expensive compression. Furthermore, it should be noted that industrial C_1 valorization involves at present the capital-intensive synthesis gas route, while a direct upgrading to intermediates of synthesis chemistry, i.e. C_{2+} olefins as building blocks, seems more attractive.

The oxidative coupling of methane into ethane and ethylene (OCM) could decrease investment costs to a large extent as neither high operating pressure nor extensive heat supply issues interfere negatively in this technology. Involving only the supply of oxygen as major feed cost factor, OCM is expected to lift major drawbacks of the natural gas to chemicals routes due to its smaller financial footprint. Furthermore, it is directly yielding value-added and easy to liquefy C_2 products well usable as base chemicals in industrial chemistry [1]. In the course of past investigations, including conventional and first combinatorial approaches, several catalyst formulations have been proposed. Providing a detailed review on past activities in OCM is beyond the scope of this work and the reader is invited to consult, e.g. the critical review on catalyst performances by Maitra [2]. One may divide explored catalysts into formulations operating at (i) rather low temperature, such as tungsten-based systems (around 400 °C) [1,4,5], and (ii) high temperature, e.g. nickel calcium oxide [6], lanthanum calcium oxide [7] or lithium magnesium oxide [8–10] based systems. It is important to stress the occurrence and importance of radical reactions proceeding in gas-phase [3] for the latter class of high-temperature catalysts. From many studies reported in literature, best C_2 selectivity and yield reached respectively 75% and 25% [11] as shown in Table 1 referring to the high-temperature domain.

Besides selecting a well-suited catalyst, advanced reaction engineering concepts like membrane reactor technology seem

---

[*] Corresponding author. Tel.: +33 472 44 5482; fax: +33 472 44 5300.
E-mail address: vanveen@ircelyon.univ-lyon1.fr (A.C. van Veen).

[1] Present address: Andre Cornelis van Veen, Ruhr University Bochum, Room NC 5/69, Universitätsstraße 150, D-44780 Bochum, Germany. Tel.: +49 234 32 24217. E-Mail: Andre.vanVeen@ruhr-uni-bochum.de.

0920-5861/$ – see front matter © 2008 Elsevier B.V. All rights reserved.
doi:10.1016/j.cattod.2008.02.024

Table 1
Performance of catalytic membrane reactors from literature

Membranes			T (°C)	Catalytic results			Reference
Type	Geom	Thickness; Ø (mm/mm)		Catalyst	CH_4 conversion (%)	Selectivity (%)	
$Bi_{1.5-x}Y_{0.5}Cu_xO_3$ $0.005 < x < 0.015$	Disk	T: 1–3; Ø: 25.5	650–850	Membrane has failed as a catalyst			[13]
$La_2Ni_{0.9}Cu_{0.1}O_3$	Disk	T: 0.6–1; Ø: 9	800–900	Pt	12.4 (850 °C)	CO: 5.2 C_2H_4: 0,16 C_2H_6: 0,57	[14]
$La_{0.6}Sr_{0.4}Co_{0.8}Fe_{0.2}O_3$	Disk	T: 0.5–2; Ø: 15.2	790–940	No catalyst	2.6–1.1	CO: 14,5 C_2H_4: 31-15 C_2H_6: 32–30	[15]
$Ba_{0.5}Sr_{0.5}Co_{0.8}Fe_{0.2}O_3$	Disk	T: 5; Ø: 17.1	800–900	No catalyst	0.5–3.5	C_2: 40–70	[16]
$BaCe_{0.8}Gd_{0.2}O_3$	Tube	$Ø_{in}$: 4.6	688–955	No catalyst	26	C_2: 62,5	[17]
$La_{0.8}Sr_{0.2}Co_{0.6}Fe_{0.4}O_3$	Disk	T: 1.85	650–950	No catalyst	17.6–18.1	C_2: 40–70	[18]
$Bi_{1.5}Y_{0.3}Sm_{0.2}O_3$	Tube	–	870–930	No catalyst	–	C_2: 54	[19]
$Ba_{0.5}Sr_{0.5}Co_{0.8}Fe_{0.2}O_3$	Tube	$Ø_{in}$: 4.5	900	No catalyst; La–Sr/CaO	10; 27	C_2: 40; C_2: 58	[21]

promising to raise performances in OCM. In the case of porous membranes distributed oxygen supply to a LaOCl catalytic membrane [12] or a Mn–W–Na/SiO_2 catalyst bed packed in a non-catalytic porous tube [20] is reported to allow for C_{2+} yields from 12 to 27.5%, respectively. However, as in both cases the porous membrane acts only as distributor, a cheap oxygen source is still required. Dense membranes with selective oxygen permeation can resolve the problem allowing the use of air for supplying pure oxygen. Several reports described the benefit of dense membranes in terms of suppressing the need of an enriched oxygen feed as well as in terms of performance [11,13–19]. Akin and Lin [11] reported in this configuration the highest C_2 yields reaching 35%. However, it should be noted that the authors used only very low methane partial pressures. Thus, it may be speculated that either the oxygen permeation rate or the catalyst performance should be improved to enhance the net productivity. The importance of catalysis over purely thermal reactions is clear as those works reporting best performances made use of efficient catalysts [21] and on the other hand choosing an unsuitable catalyst would lead to synthesis gas production [22].

Merging advantages of highly efficient catalysts and those of dense membrane reactors allows considerable savings on the oxygen supply and leads to improved performances. Thus, our laboratory started a research action on employing a well performing ionic oxygen conducting membrane enhanced by OCM catalysts. The specificities and requirements of a catalyst interacting with a dense membrane supplying oxygen directly to the catalyst lattice have been already investigated employing a model catalyst [23]. Obviously, temperature stability is a main challenge given the high operating temperature required for achieving interesting oxygen permeation fluxes. Analyzing the chemical nature of the best performing OCM catalysts, it comes that most formulations have shortcomings in terms of limited operation temperatures, lack of long-term stability or that the catalyst requires additives to the reactant feed to preserve its peak performance. Special interest in the present study is therefore devoted to performance stability.

The best systems reported in literature are lithium- lanthanum- and strontium-based catalysts [27]. Several authors demonstrated that lattice O_2^- and O_2^{2-} and adsorbed O^- species are the principal active-oxygen species for OCM [8,28–32]. The potential existence of O_2^{2-} as precursor of these lattice species has also been proposed by Zhang et al. [29].

From the obvious need to explore under comparable conditions new formulations, involving also new important criteria such as stability of catalysts at high temperatures, suitable for dense membrane application, a parallel screening approach was chosen and implemented. The overall scientific strategy of using a combinatorial approach for the development of high-performance OCM membrane reactors is exposed in Fig. 1, whereby the current work integrates in part 1. The most promising known catalysts have been selected for constituting the initial library to be screened. However, it was rapidly clear that quality of data under challenging conditions is the most important factor for selecting suitable screening equipment, given potential blank activity of reactors materials, contributions by downstream gas-phase reactions and strong heat effects at the high reaction temperatures. Thus, a novel six-channel reactor in fixed bed configuration has been developed and used in this work. The device allowed studying the influence of the chemical nature of catalysts, reaction temperature until 850 °C and a wide range of feed compositions at atmospheric pressure. More than 80 catalyst formulations have been prepared and tested within this study, using mainly MgO, CaO, and SiO_2 as supports due to their high stability. The evolution of catalysts activity after a long time on stream has also been investigated.

2. Experimental

2.1. Catalysts preparation

Catalysts were essentially prepared by four methods: incipient wetness impregnation, dry milling in an agate mortar, oxalate coprecipitation and citrates coprecipitation. Metal precursors were mainly nitrates with defined crystal water content or in dry form, purchased from Alfa-Aesar, Sigma–Aldrich and Johnson Matthey, all in a purity exceeding 99.9%. Except for the case of the dry milling method, wet mixed nitrate precursors or their defined solutions were dried for several hours at 120 °C. Then, all the materials were calcined for 6 h in air at 850 °C yielding the catalytic material. Prior to reactor charging catalysts were crushed and sieved to yield fractions in the particle size of 200–400 μm.

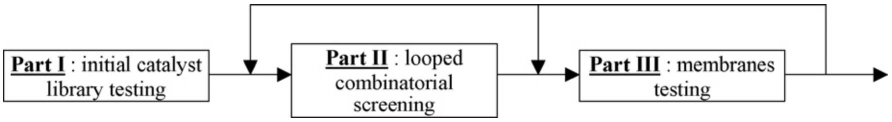

Fig. 1. Global workflow of the combinatorial OCM membrane reactor development with part I (catalyst selection from literature), part II focussing in fixed-bed parallel screening on specific parameters (temperature stability, expected membrane compatibility, and catalytic performance) and part III (validation of membrane performances and specific impact of ionic oxygen supply).

2.2. Catalyst characterization

Selected catalysts were characterized by N_2-adsorption on an ASAP 2020 instrument for obtaining the specific surface area according to the BET method, XRD pattern were recorded on a Bruker D5005 device and chemical analysis establishing the element composition was performed on Jobin Yvon Activa ICP-AES with Spectrometer D ICP-OES instrument.

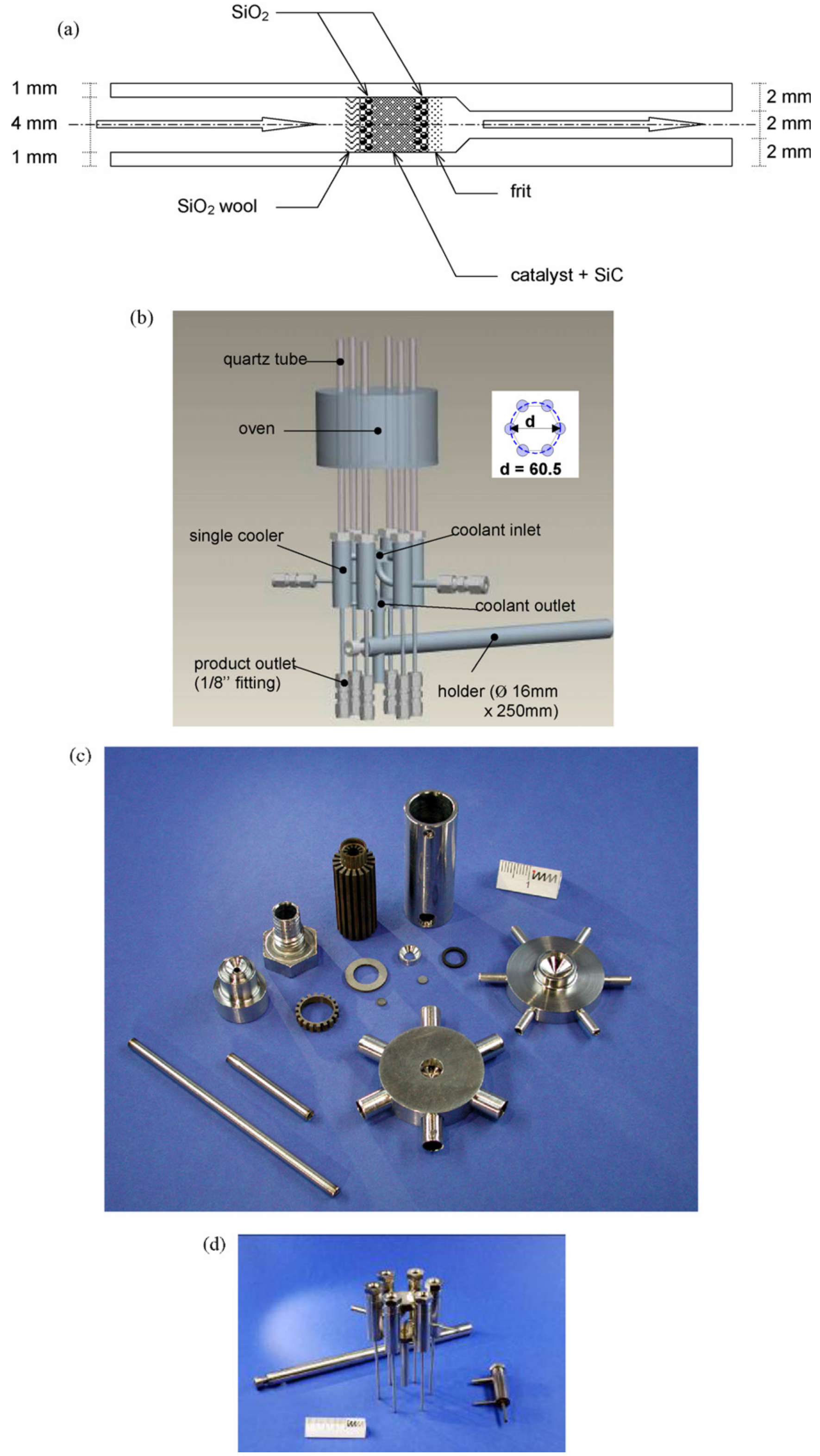

Fig. 2. Design of the parallel screening device with quench-cooler: schematic of the quartz reactor design, where arrows indicate the flow direction (contracting 20-mm long quartz tube with a frit located in the centre) (a), sketch of the 6-fold parallel reactor device provided by IMM (b), photo of the components constituting an individual quench-cooler (c) and photo of the assembled parallel quench-cooler assay for six-channel parallel screening (d).

2.3. Design and use of a 6-fold parallel reactor device

Several major technical challenges have to be faced for parallel screening at high temperatures required by OCM, namely (i) the inertness of materials in contact with reactants, (ii) the homogeneity of the temperature field where the individual channels are placed, (iii) the need to record for every channel the catalyst temperature, (iv) the suppression of secondary reactions once the fluid passed the catalytic section and finally (v) a reasonably simple use of the device. In fact, most commercial or lab-scale devices operating reasonably well at lower temperatures, like metal reactors, are unsuitable at temperatures beyond 600–700 °C as they show typically blank activity and can be polluted by previous tested formulas [49,50].

It was therefore decided to design a novel parallel screening device and benchmark it in the demanding OCM, where the presence of oxygen challenges the material inertness and the claimed participation of radical reactions [3,10] gives especial importance to a proper design of the downstream sections.

Fig. 2a depicts the schematic of a single reactor body constituting one channel. Reactors are made of quartz tubes with 6 mm external diameter and 4 and 2 mm internal diameter for inlet and outlet parts, respectively. The fixed bed containing the catalyst is maintained at its fixed position in the middle of the tube being reliably supported on a quartz frit. It should be noted that decreasing the downstream cross sectional diameter shortens the residence time of the product mixture in the reactor channel and improves the handling of the reactor, keeping especially in mind that six reactors become mounted at once in the overall device presented in Fig. 2b.

Not shown in Fig. 2, the six parallel channels are fed with the same reactant mixture and the effluent of one channel can be selected by a 6-port/2-way (5 + 1) Valco valve for analysis. The device is specifically designed to provide a zone with uniform temperature for the whole catalyst fixed bed. Thermocouples reading the precise temperature of the catalyst are inserted in an 1.5-mm diameter inconel tube itself inserted in the fixed bed, thus allowing individual measurement of reaction temperature for each catalyst.

Fig. 2 also shows the air quench-cooler/connector developed in collaboration with IMM, which prevents reactions in the effluent gases after the catalyst bed by a rapid decrease of the temperature of the reactor effluent. The quench-cooler/connector insures leak tightness even when passing very hot effluents downstream of the catalyst by the efficient cooling of O-ring seals to an uncritical level. However, holding with an electrical heating the temperature of the entire downstream section above 100 °C prevented condensation of products like water in all lines after the quench cooling.

Table 2

Literature reported performance data on various catalysts in fixed-bed configuration at atmospheric pressure

Catalyst	Support	*T* (K)	S_2 (%)	Y_2 (%)	Reference
5%(Na_2WO_4)–2% Mn (imp)	SiO_2	1093	70	20	[33]
5%(Na_2WO_4)–2% Mn (slurry)		1093	70		
5%(Na_2WO_4)–2% Mn (sol–gel)		1093	70		
30% mol Y_2O_3	Bi_2O_3	1073	46	18	[34]
5% Li	MgO	<1073	57	19.3	
NaCl–ZrO_2	ZrO_2	1073	67	24.6	[35]
LaF_3	SrO	923	57	18	[36]
SrF_2	La_2O_3	1023	58	20	
$NaZr_2(PO_4)_3$	–	1023	70	30	[37]
$Na_2Zr(PO_4)_2$	–	1023	70	30	
SrF_2	La_2O_3	1023	57.3	19.6	[38]
	Nd_2O_3	1023	57.1	19.6	
	Sm_2O_3	1073	55.8	19	
	Gd_2O_3	1023	54.6	18.8	
	Y_2O_3	1023	56.6	19	
	Eu_2O_3	1023	52.9	17.5	
	Dy_2O_3	1023	51.5	16.8	
–	Nd_2O_3	1023	57	9	[39]
5% Ni		923	69	11.5	
8% Mn		993	69	12.3	
5% Zr		1023	74	13	
BaF_2	Pr_6O_{11}	1073	57.5	19.3	[40]
	CeO_2	1073	54.6	17.6	
	Tb_4O_7	1073	56.1	18.6	
0.8% MnO_2	MgO	1023	46	17	[41]
0.35% CoO	MgO	1023	35	12	
MgO	$BaCO_3$	1053	68	16.3	[42]
La_2O_3	$BaCO_3$	1073	50	18.3	[43]
LiCl	NiO	1023	71.8	18.6	[44]
LiBr		1023	46.3	16.2	
Li–La_2O_3	MgO	973	97.8	23	[45]
Li–Ce_2O_3		973	98.4	24.6	
Li–Pr_2O_3		973	43.9	19.6	
Li–Nd_2O_3		973	95.6	23.4	
Li–Sm_2O_3		973	86.6	20.9	
$MnCl_2$	SiO_2	1023	90	13	[46]
Li–La–Mn–W	TiO_2	1043	61.7	25.6	[47]
La–Mn–W		1043	47.2	14.2	
Mn–W		1043	78.2	5.8	
Na	L_2O_3	1023	75.2	12	[48]

The O_2/CH_4 ratio in the feedstock is variable.

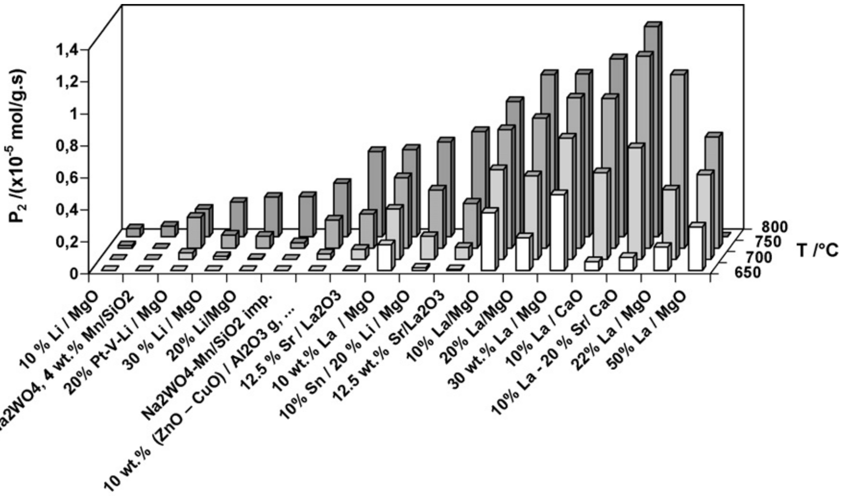

Fig. 3. C_2 productivity of active catalysts after several hours on stream.

This cooler/connector concept integrating micro-structured heat exchanger technology has several advantages, such as containing only a very small low dead volume. This feature makes the device potentially attractive for transient applications where an earliest possible and most efficient heat removal is as crucial as the preservation of the seal integrity achieved when avoiding any overheating of the O-ring seal. It should also be noted that the cooling air supplying the co-current heat exchanger is not at ambient temperature, but enters at 150 °C being chosen as operating temperature for the complete downstream section, avoiding any condensation of water formed in the reactors. Following the quench-cooler, a conventional Valco 6-port/2 way selection valve allows the computer-controlled selection of the channel to analyze. Furthermore, the choice of the analyzed channel is relayed to a homemade multiplexer unit selecting the respective thermocouple in the bed of the channel for recording.

Indeed, the choice of inconel thermocouple wells in the catalyst bed merits a commentary as the nickel containing material could induce blank activity. Test conducted under reaction condition using an inert quartz bed in the current configuration did not indicate significant activity. However, it should be noted that special care in cleaning is taken prior to each run. In fact, during the development of the reactor, both titanium as well as quartz wells were tested and eliminated due to their carbonation induced or their intrinsic fragility, respectively. Furthermore, alumina wells did not satisfy the requirement of leak tightness after several runs,

Table 3

Performance data with (Ar:CH_4:O_2) = (86.8:6.6:3.3) (a) and (Ar:CH_4:O_2) = (86.8:9.9:3.3) (b) for the best performing catalysts, both, at a total flow rate of 100 mL/min per channel and T = 800 °C

Catalyst	X_{O_2} (%)	S_2 (%)	X_{CH_4} (%)	Y_2 (%)	C_2H_6/C_2H_4	S_{CO_x} (%)	CO_2/CO	P_2 ($\times 10^{-5}$ mol/s g)
(a)								
10% La–10% Sr/CaO	97	39	32	13	0.77	61		0.75
10% La–20% Sr/CaO	92	44	37	16	0.74	56		0.75
10% La–20% Sr/CaO	97	48	43	20	0.67	52		0.96
10% La–30% Sr/CaO	89	47	31	15	0.75	53		0.86
10% La/CaO	95	40	37	15	0.7	60		0.68
10% La/CaO	97	42	41	17	0.69	58		0.79
10% La/MgO	95	29	31	9	0.71	71		0.44
10% Li/MgO	26	75	11	8	3.06	25		0.14
10% Sn–20% Li/MgO	55	51	20	10	1.44	49		0.47
10% Sn–20% Li/MgO	93	48	41	19	0.75	52		0.45
20% (Pt–V–Li)/MgO	75	48	30	14	1.24	52		0.33
20% (Pt–V–Li)/MgO	65	47	27	13	1.36	53		0.28
20% La–20% Sr/CaO	96	40	31	12	0.62	60		0.81
20% La–10% Sr/CaO	94	39	28	11	0.81	61		0.73
20% Li/MgO	34	45	7	3	2.93	55		0.16
30% Li/MgO	23	47	1	1	5.85	53		0.06
30% Li/MgO	37	57	15	8	2.05	43		0.16
5% La–20% Sr/CaO	96	46	34	16	0.65	54		0.98
5% La–30% Sr/CaO	73	53	21	11	0.98	47		0.75
5% Ni/Nd_2O_3	99	1	96	1		99	0.03	0.02
CuO–ZnO/SiO_2	91	2	23	0		98	7.03	0.02
$Fe_3Fe_4(PO_4)_6$	97	1	27	0		99	0.92	0.00
$FePO_4$	32	19	4	1		81	0.6	0.02
Mn/Nd_2O_3	97	0	25	0		100	13	0.00
(b)								
10% La–20% Sr/CaO	97	57	33	19	0.83	43		1.31
10% La/CaO	97	52	32	17	0.84	48		1.11
10% La/MgO	98	46	28	13	0.75	54		0.85
10% Li/MgO	22	69	3	2	7.56	31		0.05
10% Sn–20% Li/MgO	84	61	29	18	0.92	39		0.59
10 wt.% La/TiO_2	43	6	6	0		94	1	0.02
10 wt.% Mg/WO_3	20	1	0	0		99		0.00
10 wt.% CoO/MgO	97	0	17	0		100	11	0.00
10 wt.% La/MgO	97	34	22	8	0.91	66		0.55
12.5 wt.% Sr/La_2O_3	50	75	20	15	1.29	25		0.66
14% V/MgO	98	0	21	0		100	0	0.00
2% Pd/MgO	98	1	93	1		99	0	0.04
2% Pt/MgO	99	1	63	1		99	0	0.05
20% (Pt–V–Li)/MgO	62	46	17	8	2.03	54		0.24
20% La/MgO	96	51	28	14	0.74	49		1.01
20% Li/MgO	44	64	7	4	3.13	36		0.25
3 wt.% CuO–7 wt.% ZnO/SiO_2	78	5	12	1		95	9	0.04
30% Li/MgO	41	62	10	6	2.24	38		0.22
30 wt.% La/MgO	95	50	28	14	0.74	50		1.02
37.6 wt.% CeO_2/ZnO	97	3	17	0	1.6	97	15	0.02
5% Ni/Nd_2O_3	97	2	73	1		98	0	0.04
CuO–ZnO/SiO_2	79	4	12	1		96	6	0.04
$Fe_3Fe_4(PO_4)_6$	95	2	18	0		98	1	0.02
$FePO_4$	34	32	1	0		68	1	0.04
JM 2% Pt/Al_2O_3	98	1	61	1		99	0	0.04
La–Co–O	97	0	20	0		100	8	0.00
Mn/Nd_2O_3	97	0	17	0		100	11	0.00
Na_2WO_4–Mn/SiO_2 imp.	32	57	2	1	3.35	43		0.25
SnO_2	97	0	16	0	0.14	100	7	0.00

most probably due to a formation of micro-cracks under thermal and mechanical stress.

Products were analyzed with a mass spectrometer (Inficon IPC400) having its capillary attached right after the channel selection valve. The time resolution of data acquisition was 3 s, thus, the evolution of effluent composition could be followed almost continuously. The overall installation allowed applying experimental temperatures of more than 800 °C.

2.4. Reaction tests

The fixed bed is composed of several layers, from frit to top: one quartz particle layer, the 50 wt.% SiC–50 wt.% catalyst layer, one other quartz particle layer and one quartz wool layer. The mass of catalyst used was either 50 or 100 mg, depending on the sample density. The catalysts were supplied with a feed composed of O_2 and CH_4 diluted in Ar. The ratio O_2/CH_4 has been selected to 1:2 or 1:3. The total flow rate at the inlet of each of the six channels was 100 or 166 mL/min. The temperature of reaction has been varied from 600 to 800 °C operating all experimental runs at atmospheric pressure. The mass spectrometer product analysis used the following characteristic masses (m/e) 15 (CH_4), 26 (C_2H_4, [C_2H_6]), 27 (C_2H_4, [C_2H_6]), 28 (CO, [CO_2], [C_2H_4]), 29 (C_2H_6), 30 (C_2H_6), 32 (O_2), 40 (Ar), 44 (CO_2). Notations in brackets indicate fragment contributions of components which were subtracted during the unfolding procedure to estimate the concentration of the principal product at given m/e. This deconvolution approach proceeded according to fragmentation patterns recorded with mixtures of individual gas diluted in the internal standard Ar.

3. Results and discussion

Various authors have been describing many catalysts systems in literature but unfortunately direct comparisons are complicated as most reports use different experimental conditions or lack essential information, such as the productivity of C_{2+} products (Table 2). A first objective of this work was to establish a comprehensive collection of detailed performance data collected under similar conditions, allowing comparisons not satisfyingly possible with only given literature data. Focussing on several reference systems allows also the validation of the experimental equipment when performances established in the parallel screening coincide well with those reported in the literature.

3.1. General comparison

Fig. 3 reports the C_2-productivity (P_2) of the best catalysts in the selected initial library and proposes a direct comparison of performances obtained under similar reaction conditions, applied with the 6-fold reactor device. As a general observation, most

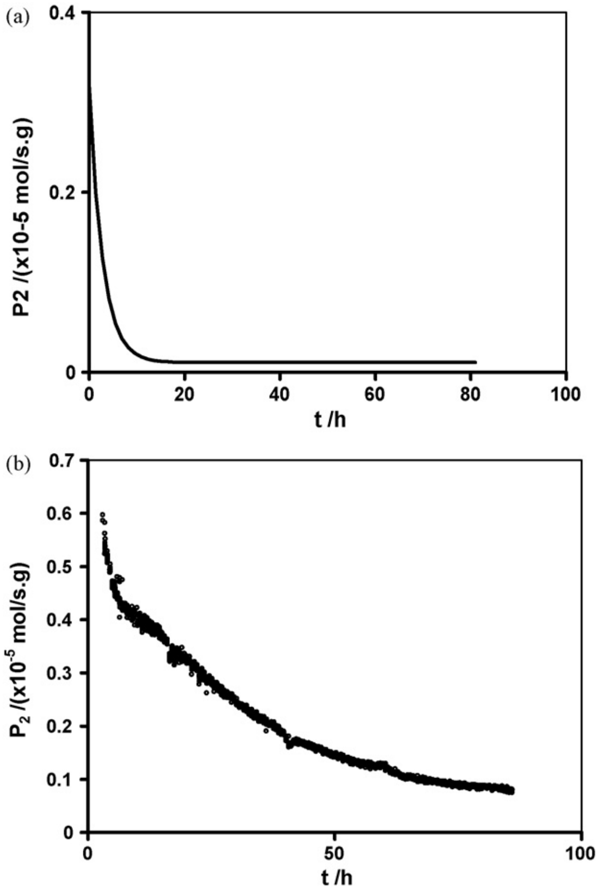

Fig. 4. Smoothed trace of C_2-productivity as a function of time for the 30% Li/MgO catalyst (a). Evolution of the C_2-productivity as a function of time for the 20% Li–10% Sn/MgO catalyst (b). Feed composition ($Ar:CH_4:O_2$) = (86.8:9.9:3.3) at a total flow rate of 100 mL/min.

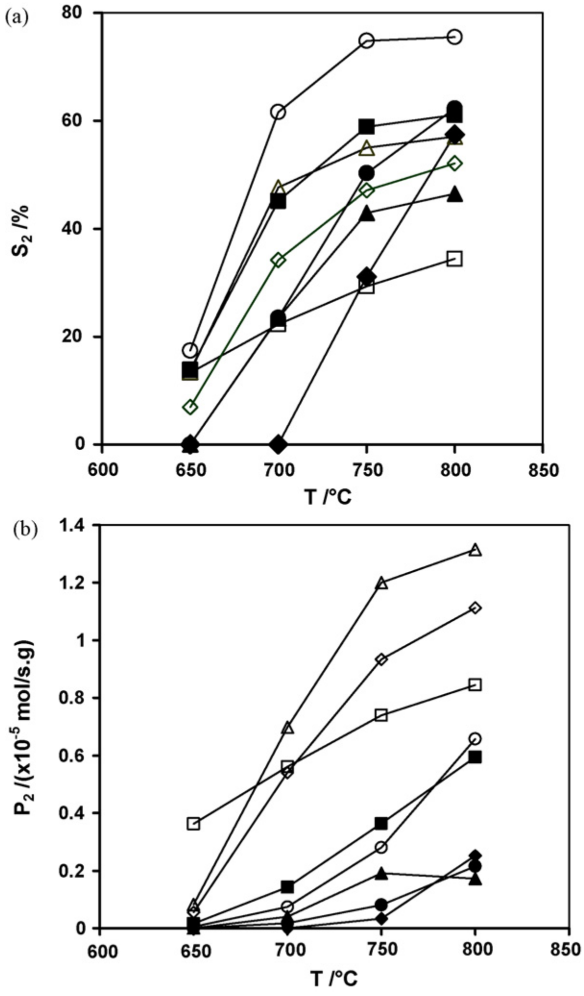

Fig. 5. C_2 selectivity (a) and C_2 productivity (b) of best catalysts as a function of temperature. Feed composition ($Ar:CH_4:O_2$) = (86.8:9.9:3.3) at a total flow rate of 100 mL/min per channel. Catalysts include: (□) 10% La/MgO; (△) 10% La–20% Sr/CaO; (◆) Na_2WO_4–Mn/SiO_2; (○) 12.5% Sr/La_2O_3; (■) 10% Sn–20% Li/MgO; (▲) 20% (Pt–V–Li)/MgO; (◇) 10% La/CaO; (●) 30% Li/MgO.

active catalysts involve MgO, CaO and La_2O_3 supports and most of these catalytic systems are also employing Li- and La-based materials, which present good performances compared to the other ones. Fig. 4 shows performances of best 10% of catalysts as a function of temperature. The common behaviour is an increase in activity and thus in C_2-productivity with temperature (tests were performed between 600 and 800 °C). The selectivity towards C_{2+} products (S_2) also increases with temperature, except for the Pt–V–Li/MgO catalyst. Table 3 reports the detailed performances of the best catalysts investigated. C_2 yields up to 10–20% could be reached with only 50 or 100 mg of catalyst. CH_4 conversion (X_{CH_4}) exceeded 30% for the best performing materials. Moreover, it should be noticed that the O_2 conversion (X_{O_2}) often reached more than 95% with those catalysts leading to highest productivity. That implies that increasing O_2 partial pressure in feed could lead to even higher CH_4 conversion and C_2 yields, especially as selectivity remained for most catalysts reasonably high. However, increasing the oxygen partial pressure was not attempted in the current configuration due to concerns operating hydrocarbon/oxygen mixtures in a parallel reactor with high-cumulated flow rates. Furthermore, the chosen conditions allow obviously in a reasonable way the comparison of widespread catalyst families ranging from noble metal systems on various supports to mixed oxide formulation.

3.2. Li-based catalysts

Li-based catalytic systems are well-known in literature [2,24,25,44–47,51,52] for their good peak performances ($S_2 > 60\%$ and $Y_2 > 25\%$) after some hours on stream. However, few investigations focussed on the stability of performance of such systems. Hence, taking benefit of the time saving parallel testing capacity, stability tests on Li-based catalysts have been performed in this study. Fig. 5 clearly indicates that the productivity of 30% Li/MgO and 10% Li–20% Sn/MgO declines after 10–20 h of reaction and after 90 h on stream, these catalysts are essentially no longer active. A comparable behaviour has been observed for all other Li-containing catalysts.

Investigating the strong deactivation phenomenon of Li-based catalysts it was observed that the performance loss is paralleled by a decline in the Li concentration in the catalyst, most probably caused by the volatile character of the Li compounds formed under OCM conditions, in agreement with [25,52]. Chemical analysis of

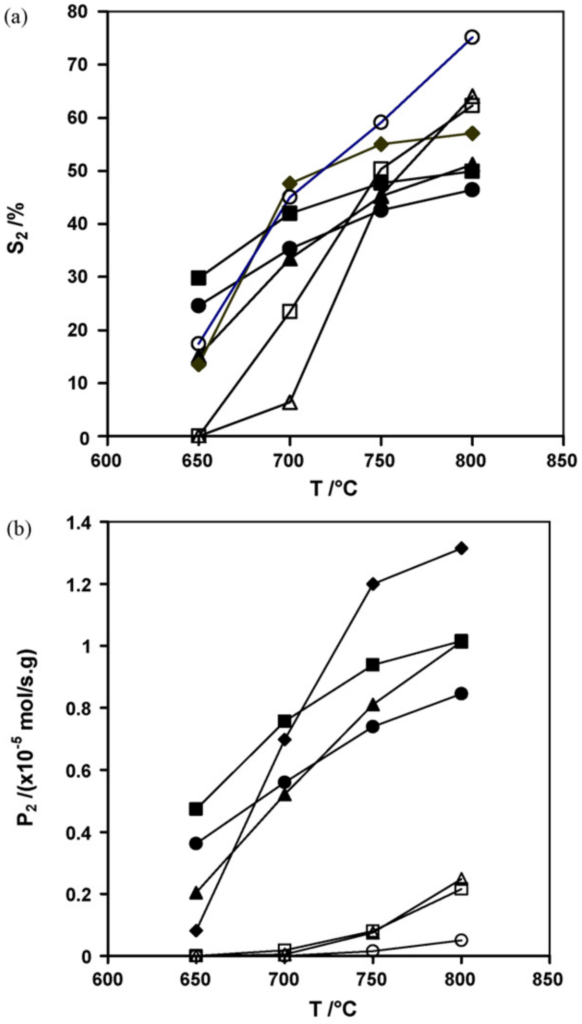

Fig. 6. C_2 selectivity (a) and C_2 productivity (b) of La- and Li-based catalysts at different loadings as a function of temperature after several hours on stream. Feed composition ($Ar:CH_4:O_2$) = (86.8:9.9:3.3) at a total flow rate of 100 mL/min per channel. Catalysts include: (△) 10% Li/MgO; (□) 20% Li/MgO; (○) 30% Li/MgO; (▲) 10% La/MgO; (■) 20% La/MgO; (●) 30% La/MgO.

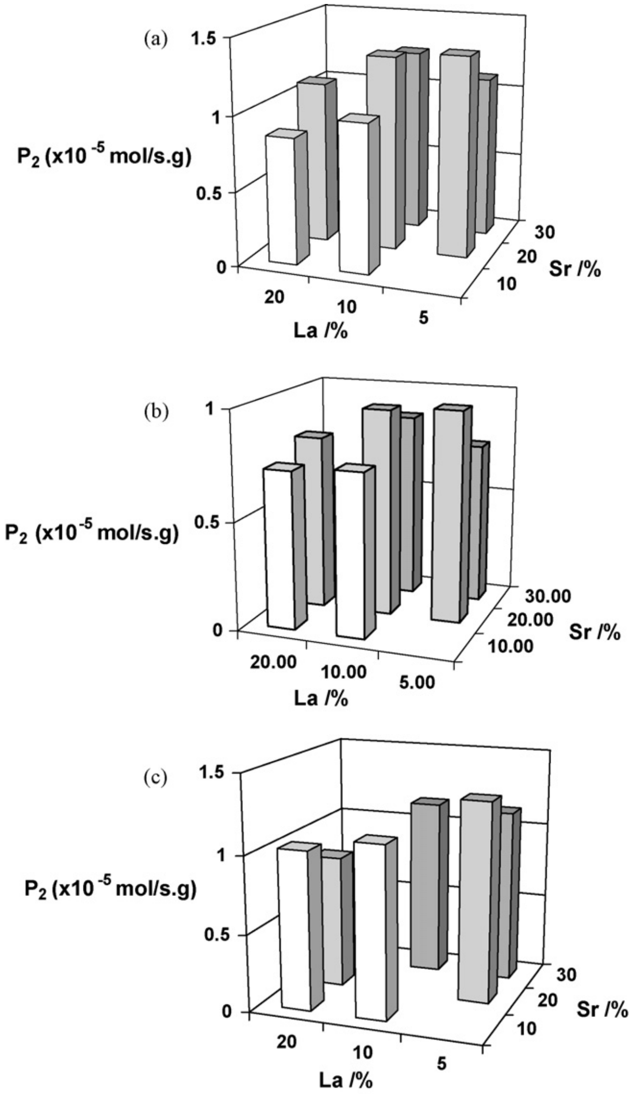

Fig. 7. C_2 productivity of LaSr/CaO catalysts at 800 °C as a function of the La and Sr contents observed at a total flow rate of 100 mL/min per channel for feed compositions of ($Ar:CH_4:O_2$) = (87.8:9.9:3.3) (a), (90.1:6.6:3.3) (b) and (85:10:5) (c).

Table 4
La–Sr/CaO catalyst performances with a reactant feed of ($Ar:CH_4:O_2$) = (90.1:6.6:3.3) (a), ($Ar:CH_4:O_2$) = (85:9.9:3.3) (b) and ($Ar:CH_4:O_2$) = (85:10:5) (c) all at a total flow rate of 100 mL/min and T_{oven} = 800 °C

Catalyst	Performances						
	X_{O_2} (%)	S_2 (%)	X_{CH_4} (%)	Y_2 (%)	C_2H_6/C_2H_4	S_{CO_2} (%)	P_{C_2} ($\times 10^{-5}$ mol/s g)
(a)							
10% La–10% Sr/CaO	96	39	32	12	0.77	61	0.75
10% La–20% Sr/CaO	97	47	42	20	0.67	52	0.96
10% La–30% Sr/CaO	88	47	31	14	0.75	52	0.86
20% La–10% Sr/CaO	94	38	27	10	0.81	61	0.73
5% La–20% Sr/CaO	96	46	34	15	0.65	53	0.98
5% La–30% Sr/CaO	73	52	21	11	0.98	47	0.75
20% La–20% Sr/CaO	96	40	30	12	0.62	59	0.81

Catalyst	Performances						
	X_{O_2} (%)	S_2 (%)	X_{CH_4} (%)	Y_2 (%)	C_2H_6/C_2H_4	S_{CO} (%)	P_{C_2} ($\times 10^{-5}$ mol/s g)
(b)							
10% La–10% Sr/CaO	96	46	19	9	0.95	53	0.99
10% La–20% Sr/CaO	96	57	33	19	0.83	43	1.31
10% La–30% Sr/CaO	90	57	19	11	0.88	46	1.25
20% La–10% Sr/CaO	96	42	17	7	1.02	57	0.85
5% La–20% Sr/CaO	96	56	24	13	0.83	44	1.35
5% La–30% Sr/CaO	79	60	15	9	1.09	39	1.10
20% La–20% Sr/CaO	96	48	19	9	0.74	51	1.10

Catalyst	Performances						
	X_{O_2} (%)	S_2 (%)	X_{CH_4} (%)	Y_2 (%)	C_2H_6/C_2H_4	S_{CO_x} (%)	P_{C_2} ($\times 10^{-5}$ mol/s g)
(c)							
10% La–10% Sr/CaO	97	32	28	9	0.91	68	0.86
10% La–30% Sr/CaO	85	50	27	14	0.73	50	1.30
20% La–10% Sr/CaO	97	37	29	11	0.78	63	1.02
20% La–20% Sr/CaO	97	38	28	11	0.63	62	1.10
5% La–20% Sr/CaO	94	41	30	13	0.92	59	1.14
5% La–30% Sr/CaO	70	54	20	11	0.96	46	1.12
20% La–20% Sr/CaO	97	38	28	11	0.63	62	1.10

samples collected after reaction indicates that Li amount is divided by a factor of 4–5 compared to the initial quantity, confirming the loss of Li. It should be mentioned that a decreased performance stability of Li/MgO catalysts using quartz as reactor material presents a known issue [52]. On the other hand, even using alternative materials like dense alumina, presenting for the proposed parallel reactor the inconvenience of missing transparency and thus a complication for positioning the thermocouple well, did not entirely prevent declining performances due to Li losses. This catalytic system is therefore not suitable for an industrial process involving high-temperature operation in a dense membrane reactor. Wong et al. [53] reported good performances such as $S_2 > 65\%$ and $Y_2 > 20\%$ on a 3% Na_2O–9% $La_2O_3/BaCO_3$ catalyst, but as Na can be considered as volatile as Li, the same deactivation phenomenon due to evaporation is expected leading to a poor stability of the catalyst.

3.3. La-based catalysts

The other active catalyst family cited in literature [26,30,36,47,54] and also confirmed in this study is that of La-based catalysts. Peak performances comparable to the ones reported in literature have been obtained with these catalysts. A Stability study shows that even after 90 h of reaction, the activity of such catalysts remains quite high. Fig. 6 compares the performances of Li- and La-based catalysts. Li-based catalysts are clearly less efficient than La-based ones with an equal promoter loading, but it should be kept in mind that Li evaporation occurs quickly enough to modify the effective Li load for Li/MgO catalysts. However, C_2-selectivity (S_2) easily reaches 40–60% for La/MgO and Li/MgO catalysts and even more than 75% for LaSr/CaO systems.

3.4. LaSr/CaO system optimisation

Although LaSr/CaO is remarkably performing and stable OCM catalyst, it has been hardly studied in a systematic way and no exhaustive investigation on this catalyst class is reported. Having identified such formulations as highly promising, several compositions of this type have been tested. Moreover, missing information on the most suitable operating conditions, those samples were submitted to different reaction conditions in a wider screening approach in order to investigate the best composition and individual role of elements in this promising catalyst class under different conditions. Table 4 and Fig. 7 show the compositions and performances of LaSr/CaO catalysts. The best results are obtained with 5% La–20% Sr/CaO and 10% La–20% Sr/CaO with a feed composed of ($Ar:CH_4:O_2$) = (85:9.9:3.3). Obviously, La is strongly involved in the oxygen activation, most likely via carbonates formation/decomposition over surface defects [17], but selectivity remains comparably low when this element dominates the catalyst formulation. Given the observation in Fig. 7, an action of Sr as moderator is highly probable, i.e. this element is enhancing selectivity. Finally, in line with the MgO performance, CaO is a high-temperature stable basic catalysts support.

3.5. Kinetic features

Fig. 8 shows the behaviour of peak S_2 with CH_4 conversion over La-based catalysts. The different X_{CH_4} values are obtained at

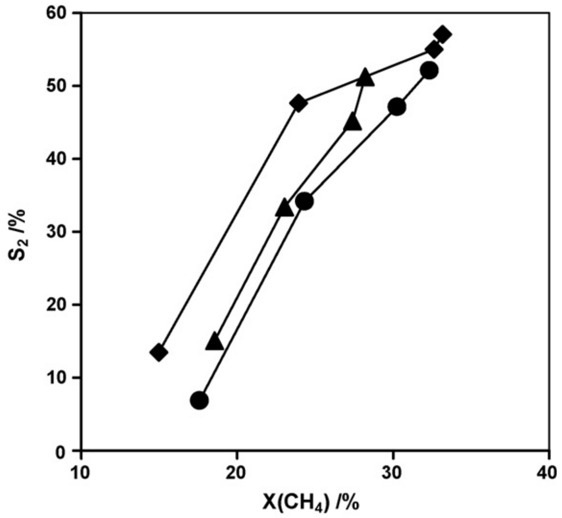

Fig. 8. C_2 selectivity of best performing catalysts at different methane conversions after several hours on stream using a feed composition of ($Ar:CH_4:O_2$) = (86.8:9.9:3.3) and a total flow rate of 100 mL/min per channel. Catalyst samples include: (◆) LaSr/CaO; (●) 10% La/CaO; (▲) 20% La/MgO.

reaction temperatures ranging from 600 to 800 °C. It is obvious that a catalyst system with small variations of selectivity would be preferable for industrial exploitation purposes as up-scaling becomes greatly facilitated when the degree can be enhanced without severe losses in selectivity. One feature seems quite remarkable, namely the tendency that rising X_{CH_4} leads to higher S_2 (more than 30% and more than 55%, respectively). First from a purely practical point of view, this indicates that performances can still be enhanced increasing the concentration of O_2 in the feed. Secondly, this behaviour seems linked to the very high O_2 consumption (more than 95%) reported under these conditions, confirming the aspect of an insufficient O_2 supply for the best performing samples in respect to the applied standard conditions applied for all benchmarking in the present parallel screening study. It seems reasonable that initially formed C_{2+} products could deteriorate over remaining catalyst once the initially supplied oxygen is consumed. However, it should be noted that this is a generic problem of all parallel testing as soon as vastly spread catalyst libraries become employed, which obviously require for comparison reasons compromises the testing conditions applied to the entire set of catalysts. However, it is deemed that the ratio ($O_2:CH_4$) = (1:3) fixed in the initial screening strategy allows a reasonable performance ranking and that that a reasonable trade-off between comparability among all the various catalysts and experimental effort consists in altering the ($O_2:CH_4$) ratio only for a more restricted screening of lead candidates. Fig. 9 shows the influence of the (O_2/CH_4) ratio in feed on peak P_2 for the La-based catalysts. As expected from earlier kinetic studies, the higher this ratio is, the lower the selectivity, despite the stoichiometry of ($O_2:CH_4$) = (1:2) in OCM, which allows expecting better performances with a 0.5 ratio than with a 0.3 ratio once unselective contributions become suppressed. On the other hand, there seems existing a clear tendency that reactant methane partial pressures favour performances and the slightly decreased CH_4 concentration in the feedstock could explain the decrease in performances. One might speculate that the literature reported contribution of gas-phase radical reaction are at the origin of performance enhancements with less diluted reactant feeds, but obviously further complementary studies beyond a parallel screening are needed to evaluate more in detail the influence of CH_4 and O_2 concentrations.

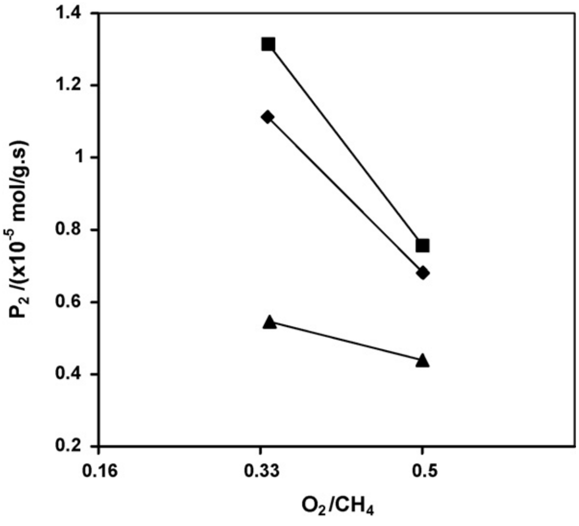

Fig. 9. Variation of C_2 productivity of best performing catalysts as a function of the O_2/CH_4 ratio at a total flow of 100 mL/min per channel and a feed composition ($Ar:CH_4:O_2$) = (86.8:9.9:3.3) and ($Ar:CH_4:O_2$) = (90.1:6.6:3.3). Catalyst samples include: (▲) 10% La/MgO; (◆) 10% La/CaO; (■) 10% La–20% Sr/CaO.

4. Conclusions

A wide panel of catalysts for the OCM reaction has been tested with a novel 6-fold screening device for selecting adapted formulas in view of an use in dense membrane reactors. The combinatorial 6-fold reactor allowing precise temperature measurement was validated and inertness could be achieved due to the suppression of wall effects, i.e. blank activity. The quench-cooler/connector device combined with suitably designed quartz reactor channels avoided detrimental gas-phase reactions downstream of the catalyst, thus allowing precise quantitative analysis of catalyst performances based on the effluent gases composition. The influence of various parameters such as feeding composition, reaction temperature and reaction duration on catalytic performances has been investigated. Good C_2 yield and productivity were obtained with La-based catalysts such as 10 wt.% La–20 wt.% Sr/CaO, La/CaO without any noticeable decrease in activity after several hours of reaction. Performances were even superior to those reported for such catalysts previously in literature [21]. Although Li-based catalysts also showed very good performances during the first hours of reaction, the activity decreases drastically after longer times, probably because a loss of Li during operation.

Finally, a better control of O_2 feeding and of gas-phase reactions seems highly suitable for improving the comprehension of the reaction mechanism and maximization catalyst performances. The high thermal stability of the La–Sr/CaO system underlines the potential for employing this type catalyst in another reactor design, such as a dense membrane reactor, which seems extremely promising in further OCM studies.

Acknowledgements

The study is supported by the European research project “TOPCOMBI” (contract NMP2-CT2005-515792).

References

[1] U. Rodemerck, P. Ignaszewski, M. Lucas, P. Claus, Chem. Eng. Technol. 23 (2000) 413.
[2] A.M. Maitra, Appl. Catal. A: Gen. 104 (1993) 11.

[3] V.I. Vedeneev, O.V. Krylov, V.S. Arutyunov, V.Ya. Basevich, M.Ya. Goldenberg, M.A. Teitel boim, Appl. Catal. A: Gen. 127 (1995) 51.
[4] A. Malekzadeh, A. Khodadadi, M. Abedini, M. Amini, A. Bahramian, A.K. Dalai, Catal. Commun. 2 (2001) 241.
[5] A. Malekzadeh, M. Abedini, A.A. Khodadadi, M. Amini, H.K. Mishra, A.K. Dalai, Catal. Lett. 84 (2002) 45.
[6] A. Toebes, K.M. Dooley, J.R.H. Ross, Catal. Today 21 (1994) 401.
[7] D. Schweer, L. Mleczko, M. Baerns, Catal. Today 21 (1994) 357.
[8] C. Mirodatos, G.A. Martin, J.C. Bertolini, J. Saint-Just, Catal. Today 4 (1989) 301.
[9] G.C. Hoogendam, K. Seshan, J.G. van Ommen, J.R.H. Ross, Catal. Today 21 (1994) 333.
[10] Q. Chen, P.M. Couwenberg, G.B. Marin, Catal. Today 21 (1994) 309.
[11] F.T. Akin, Y.S. Lin, Catal. Lett. 78 (2002) 239.
[12] H. Borges, A. Giroir-Fendler, C. Mirodatos, P. Chanaud, A. Julbe, Catal. Today 25 (1995) 377.
[13] J. Han, Y. Zeng, Y.S. Lin, J. Mem. Sci. 132 (1997) 235.
[14] V.V. Kharton, A.A. Yaremchenko, E.V. Tsipis, A.A. Valente, M.V. Patrakeev, A.L. Shaula, J.R. Frade, J. Rocha, Appl. Catal. A: Gen. 261 (2004) 25.
[15] J.E. ten Elshof, H.J.M. Boumeester, H. Verweij, Appl. Catal. A: Gen. 130 (1995) 195.
[16] Z.P. Zhao, H. Dong, G. Xiong, Y. Cong, W. Yang, J. Mem. Sci. 183 (2001) 181.
[17] Y. Lu, A.G. Dixon, W.R. Moser, Y.H. Ma, U. Balachandran, J. Mem. Sci. 170 (2000) 27.
[18] Y. Zeng, Y.S. Lin, S.L. Swartz, J. Mem. Sci. 150 (1998) 87.
[19] F.T. Akin, Y.S. Lin, AIChE J. 48 (2002) 2298.
[20] Y. Lu, A.G. Dixon, W.R. Moser, Y.H. Ma, Chem. Eng. Sci. 55 (2000) 4901.
[21] H. Wang, Y. Cong, W. Yang, Catal. Today 104 (2005) 160.
[22] A.A. Yaremchenko, A.A. Valente, V.V. Kharton, E.V. Tsipis, J.R. Frade, E.N. Naumovich, J. Rocha, F.M.B. Marques, Catal. Lett. 91 (2003) 169.
[23] S. Haag, A.C. van Veen, C. Mirodatos, Catal. Today 127 (2007) 157.
[24] J.H. Lunsford, Catal. Today 6 (1990) 235.
[25] G.A. Martin, C. Mirodatos, Morphological aspects of catalysts for oxidative coupling of methane, in: E.E. Wolf (Ed.), Methane Conversion by Oxidative Processes, Van Nostrand Reinhold, New York, 1992, pp. 351–381.
[26] S. Lacombe, C. Geantet, C. Mirodatos, J. Catal. 151 (1995) 439.
[27] V.R. Choudhary, S.A.R. Mulla, B.S. Uphade, Fuel 78 (1999) 427.
[28] J.H. Lunsford, Angew. Chem. Int. Ed. Engl. 34 (1995) 970.
[29] H.B. Zhang, G.D. Lin, H.L. Wan, Y.D. Liu, W.Z. Weng, J.X. Cai, Y.F. Shen, K.R. Tsai, Catal. Lett. 73 (2001) 2.
[30] C.T. Au, T.-J. Zhou, W.-J. Lai, C.-F. Ng, Catal. Lett. 49 (1997) 53.
[31] K.D. Campbell, E. Morales, J.H. Lunsford, J. Am. Chem. Soc. 109 (1987) 7900.
[32] M. Hatano, K. Otsuka, J. Chem. Soc. Faraday Trans. 85 (1989) 199.
[33] J. Wang, L. Chou, B. Zhang, H. Song, J. Zhao, J. Yang, S. Li, J. Mol. Catal. A: Chem. 245 (2006) 272.
[34] Y. Zeng, Y.S. Lin, Appl. Catal. A: Gen. 159 (1997) 101.
[35] K.J. Yoon, H.L. Tung, Appl. Catal. A: Gen. 159 (1997) 59.
[36] R.-Q. Long, S.-Q. Zhou, Y.-P. Huang, W.-Z. Weng, H.-L. Wan, K.-R. Tsai, Appl. Catal. A: Gen. 133 (1995) 269.
[37] K.J. Yoon, S.W. Seo, Appl. Catal. A: Gen. 161 (1997) L5.
[38] R. Long, Y. Huang, W. Weng, H. Wan, K. Tsai, Catal. Today 30 (1996) 59.
[39] S.H. Lee, D.W. Jung, J.B. Kim, Y.-R. Kim, Appl. Catal. A: Gen. 164 (1997) 159.
[40] R. Long, J. Luo, M. Chen, H. Wan, Appl. Catal. A: Gen. 159 (1997) 171.
[41] T.K. Chan, K.J. Smith, Appl. Catal. 60 (1990) 13.
[42] J. Da, X. Ding, S. Shen, Appl. Catal. A: Gen. 116 (1994) 81.
[43] Z.-L. Zhang, C.T. Au, K.R. Tsai, Appl. Catal. 62 (1990) L29.
[44] K. Otsuka, Q. Liu, A. Morikawa, Inorg. Chim. Acta 118 (1986) L23.
[45] B. Yingli, Z. Kaiji, J. Yutao, T. Chiwen, Y. Xiangguong, Appl. Catal. 39 (1988) 185.
[46] T.R. Baldwin, R. Burch, E.M. Crabb, G.D. Squire, S.C. Tsang, Appl. Catal. 56 (1989) 219.
[47] M.-C. Gong, X.-H. Xu, Y.-Q. Chen, J.-L. Zhou, Y. Chen, Catal. Today 24 (1995) 263.
[48] M. Yamamura, H. Okado, N. Tsuzuki, T. Wakatsuki, K. Otsuka, Appl. Catal. A: Gen. 122 (1995) 135.
[49] X.-Q. Qiu, Q.-M. Zhu, N.-B. Wong, K.-C. Tin, J. Chem. Tech. Biotechnol. 65 (1996) 380.
[50] G. Morra, A. Desmartin-Chomel, C. Daniel, U. Ravon, D. Farrusseng, R. Cowan, M. Krusche, C. Mirodatos, High-throughput gas phase transient reactor for catalytic material characterization and kinetic studies, Chem. Eng. J. 138 (2008) 379.
[51] X.-Q. Qiu, N.-B. Wong, K.-C. Tin, Q.-M. Zhu, J. Chem. Tech. Biotechnol. 65 (1996) 303.
[52] S.J. Korf, J.A. Roos, N.A. de Bruijn, J.G. van Ommen, J.R.H. Ross, Appl. Catal. 58 (1990) 131.
[53] N.-B. Wong, K.-C. Tin, K. Lau, J. Chem. Tech. Biotechnol. 65 (1996) 351.
[54] S. Lacombe, H. Zanthoff, C. Mirodatos, J. Catal. 155 (1995) 106.